A Simple Patch Antenna Design with Multiple Linear Polarizations for RFID Readers

Trang Hoang-Thu, Hung Pham-Duy, Hung Tran-Huy, and Hyun-Chang Park

***Abstract*—This paper proposed a compact antenna with multiple linear polarization realization for radio frequency identification (RFID) operating at ultra-high frequency (UHF) band. The main radiator is a crossed patch, which is excited by different feeding positions to adjust the current flowing on the patch. To minimize the unwanted effect of the biasing circuit on the antenna radiation performance, the antenna is excited through a reconfigurable feeding network with one input and three outputs. By controlling the ON/OFF states of three PIN diodes integrated into the feeding network, four different modes including horizontal, vertical, and both diagonal polarizations can be realized. The final antenna design with overall dimensions of $0.67\,\lambda \times 0.67\,\lambda \times 0.04\,\lambda$ at 915 MHz shows good matching performance from 910 to 925 MHz. Within this band, the broadside gain values for all polarization states are better than 6.2 dBi.**

Link to graphical and video abstracts, and to code:
https://latamt.ieeer9.org/index.php/transactions/article/view/10622

***Index Terms*—RFID Antenna, Ultra-High Frequency, Linear Polarization, Reconfigurable Antenna, PIN Diode, Crossed Patch Antenna, Polarization Diversity.**

I. Introduction

ANTENNAS are fundamental components of Radio Frequency Identification (RFID) systems, as they directly determine how efficiently information is transferred between the reader and the tag. Their role extends beyond simple transmission and reception; they critically influence the operating range, reliability, and overall system performance [1]. Since RFID tags are typically linearly polarized (LP), various antennas with LP realization have been proposed [2]–[6]. However, polarization mismatch might occur between the randomly oriented tags and readers. Accordingly, circularly polarized (CP) antenna is commonly employed to maintain reliable communication. In [7]–[9], the authors have proposed CP antenna designs with fixed polarization state, either right-hand CP (RHCP) or left-hand CP (LHCP). For better performance, dual-CP antennas are also reported in [10]–[12].

However, the use of CP reader inherently introduces a 3 dB polarization mismatch loss—corresponding to a 50% reduction in power transfer between the reader and the commonly LP tag. Polarization reconfigurable antennas improve RFID reader performance by minimizing polarization mismatch, enabling more reliable tag detection and longer reading range. Their adaptability enhances multi-tag reading in complex environments while reducing hardware complexity and overall system size. In [13], [14], antennas with capable of switching between CP and LP states are proposed. Nevertheless, such approaches may still encounter polarization inefficiencies under certain tag orientations.

To mitigate this loss, multiple-linearly polarized reconfigurability has been proposed. Multiple LP reconfigurable antenna can be conveniently produced by using dipole structures [15], [16] produce four polarization states at a rotation angle of $45°$. Nonetheless, high profile is the critical drawback of such antennas. A thorough investigation indicates that very few antennas have been reported that can switch among multiple LPs [17]–[19].

Overall, to achieve polarization reconfigurability, the common method is to attach various PIN diodes into the radiating element [20]–[24]. However, both diodes and their biasing circuitry can introduce unwanted radiation that distorts the antenna's intended pattern. To address this limitation, an alternative approach for polarization reconfigurability is to utilize switchable feeding networks [25]–[29].

This paper presented a simple design of reconfigurable antenna, whose polarization can be altered among horizontal, vertical, and both diagonal polarization states. The polarization switching capability is based on a reconfigurable feeding network. It is noted that four different LP modes can be realized by controlling the ON/OFF states of just three PIN diodes. This simple switching mechanism is much simpler than the other related works. The proposed antenna shows good operation characteristics in the frequency range from 900 to 920 MHz.

II. Antenna Design

Fig. 1 illustrates the geometrical configuration of the proposed polarization-reconfigurable antenna. The structure is implemented using two low-cost FR-4 substrates (dielectric constant 4.4 and loss tangent 0.02). These two substrates are separated by an air gap layer. Noted that the antenna thickness significantly influences the achievable operating bandwidth. In this design, the overall thickness is selected to be approximately 10 mm in order to obtain the desired operating bandwidth. The main radiator of crossed-patch radiator is etched on the top surface of the upper substrate, whereas the reconfigurable feeding network is printed on the underside of

The associate editor coordinating the review of this manuscript and approving it for publication was Roberto S. Murphy (*Corresponding author: Hung Tran-Huy*).

T. Hoang-Thu, H. Pham-Duy, and Hung Tran-Huy are with the Faculty of Electrical and Electronic Engineering, PHENIKAA School of Engineering, PHENIKAA University, Hanoi 12116, Vietnam (e-mails: 21013356@st.phenikaa-uni.edu.vn, hung.phamduy@phenikaa-uni.edu.vn, and hung.tranhuy@phenikaa-uni.edu.vn).

H. C. Park is with the Division of Electronics & Electrical Engineering, Dongguk University, Seoul, Korea (e-mail:hcpark@dongguk.edu.vn).

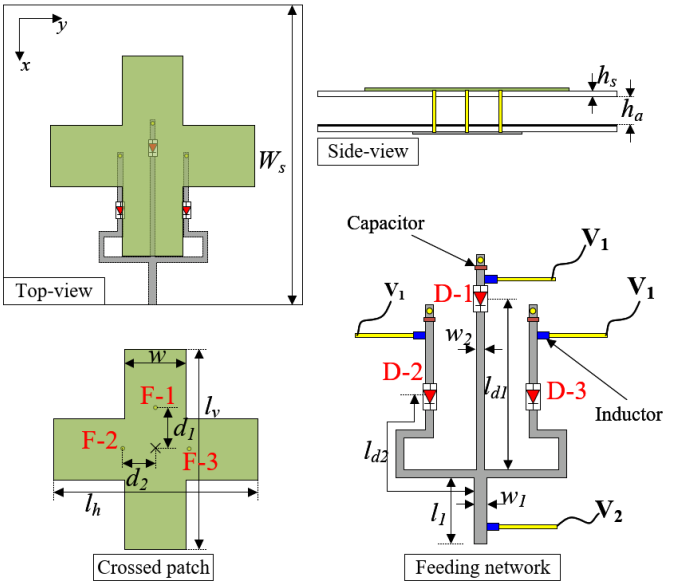

Fig. 1. Geometrical configuration of the proposed polarization reconfigurable antenna.

the lower substrate. Polarization switching among multiple LPs is achieved through three PIN diodes type MACOM MADP-042305-130600 integrated into a one-to-three power divider. These diodes, labeled D-1, D-2, and D-3, share a common cathode configuration. By selectively activating the diodes, the crossed patch can be excited at three distinct feed points, denoted F-1, F-2, and F-3, thereby enabling multiple LP states with interval of $45°$.

For biasing, four 200-nH inductors are employed, which act as the RF choke to prevent RF current flowing from the divider to the biasing circuit. Three 200 pF capacitors are employed to block the DC current. Therefore, the ON/OFF states of three PIN diodes can be controlled independently by using two different voltage sources, V_1 and V_2. When D-1 is connected to the V_1 source, D-1 is switched ON while the others are switched OFF. Meanwhile, D-1 and D-2 are activated when connecting both to V_1. Noted that according to the datasheet [30] the ON state of the diode is equivalent to a resistor of $1.32\,\Omega$, while the OFF state is equivalent to a capacitor of 0.15 pF.

The antenna is characterized by using the Ansys High Frequency Structure Simulator (HFSS) with lumped port excitation. The optimized geometric parameters of the proposed polarization-reconfigurable antenna are summarized as follows: $W_s = 220$, $h_s = 1.6$, $h_a = 10$, $l_v = 147$, $l_h = 150$, $d_1 = 28$, $d_2 = 24$, $w_1 = 5.6$, $w_2 = 3.8$, $w = 45$, $l_1 = 31$, $l_{d1} = l_{d2} = 80$ (unit: mm).

It is worth noting that the horizontal arm connected to D-2 and D-3 through two pins, which are connected in a parallel configuration. Meanwhile, the vertical arm connected to D-1 through one pin. Thus, the inductance produced by the pins of when the horizontal arm is excited will be smaller than the other case. Thus, when the vertical and horizontal arms have similar length, the resonance of the horizontal arm will be higher than that of the vertical arm. To make these resonances identical, the horizontal arm should be slightly longer than the vertical arm. As the input impedance of the patch changes from 0-ohm at the center to infinite at the edge. Moving the feeding position along the resonant length of the patch can achieve good impedance matching. Meanwhile, the resonant length of the patch is determined by equations (1) and (2):

$$\varepsilon_{eq} = \frac{h_s + h_a}{\frac{h_s}{\varepsilon_{FR-4}} + \frac{h_a}{\varepsilon_{air}}} \tag{1}$$

$$l = \frac{c}{2f\sqrt{\varepsilon_{eq}}} \tag{2}$$

III. Antenna Operation Characteristics

The polarization switching mechanism of the proposed antenna is achieved by selectively activating the excitation points F-1, F-2, and F-3 on the crossed patch. The corresponding polarization states for each diode configuration are summarized in Table I. For instance, when only D-1 is turned ON, the antenna generates vertical polarization, whereas activating only D-2 produces horizontal polarization. Similarly, enabling D-1 and D-2 while disabling D-3 results in a $+45°$ linear polarization, whereas turning ON D-1 and D-3 with D-2 OFF yields a $-45°$ polarization state.

TABLE I
Polarization Corresponding to the Diode States

D-1	D-2	D-3	Feeding positions	Operating mode	Schematic ($V_1 > V_2$)
OFF	ON	OFF	F-2	Horizontal pol.	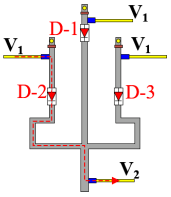
ON	OFF	OFF	F-1	Vertical pol.	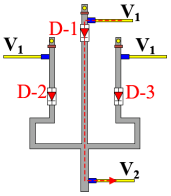
ON	ON	OFF	F-1 and F-2	+45° pol.	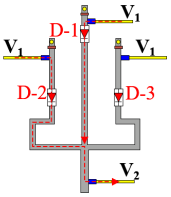
ON	OFF	ON	F-1 and F-3	-45° pol.	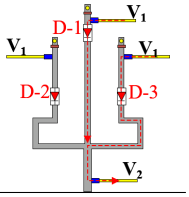

The simulated reflection coefficient $|S_{11}|$ results for different polarization states are depicted in Fig. 2. It can be seen

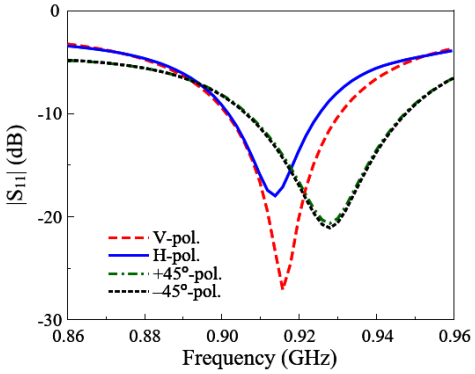

Fig. 2. Simulated $|S_{11}|$ for different operating modes.

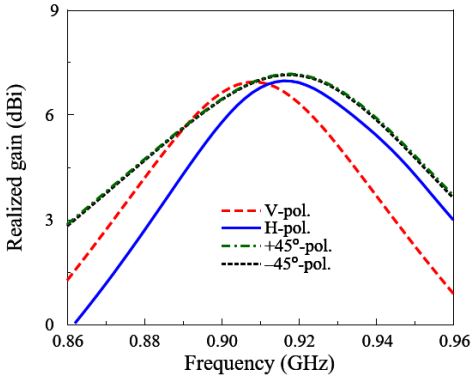

Fig. 3. Simulated broadside gain for different operating modes.

obviously that there is a slightly different in terms of -10 dB impedance bandwidth of different modes. The common operating bandwidth, in which the $|S_{11}|$ of all polarization states are all below -10 dB, is from 900 to 920 MHz.

The simulated broadside gains of such operating modes are shown in Fig. 3. As seen, the broadside gain values are all better than 5.8 dBi across the operational bandwidth (905–926 MHz). Maximum gain of 7.2 dBi is achieved at 915 MHz for diagonal polarization states. Noted that the the realized gain is considered in the broadside direction, in which $\varphi = 0°$ and $\theta = 0°$. For vertical and horizontal polarizations, the maximum gain will be in the broadside direction. In the diagonal polarization modes, both the vertical and horizontal arms of the crossed patch are excited simultaneously. Due to the slight difference in the lengths of these arms, as well as the small length difference between the feeding branches associated with F-1 and F-2 (or F-3), a minor phase imbalance may occur. Consequently, the direction of maximum gain may be slightly tilted away from the exact broadside direction.

The radiation pattern at 910 MHz for all polarization states are plotted in Fig. 4. Both co-polarization and cross-polarization characteristics in the principal E- and H-planes are evaluated. The results show that the antenna maintains symmetrical broadside radiation patterns for all polarization states. The polarization isolation - defined as the gain difference between the co-polarized and cross-polarized components in the broadside direction - exceeds 15 dB. In addition, the front-to-back ratio, valued by the gain contrast between the forward and backward directions, is also greater than 15 dB.

The polarization behavior of the proposed antenna is further validated by examining the simulated vector J-field distributions on the crossed patch at 910 MHz, as illustrated in Fig. 5. The J-field vectors are observed at multiple phase intervals to capture the polarization orientation over a full excitation cycle. When a single diode is activated, the J-field exhibits a consistent linear orientation - horizontal for one excitation path and vertical for the other - confirming the generation of the corresponding LP states. In contrast, when two diodes are turned ON simultaneously, the J-field vectors align along the diagonal axes of the crossed patch, thereby producing the $+45°$ and $-45°$ linear polarization states. These results clearly demonstrate the antenna's capability to achieve four distinct polarization modes through diode-controlled excitation.

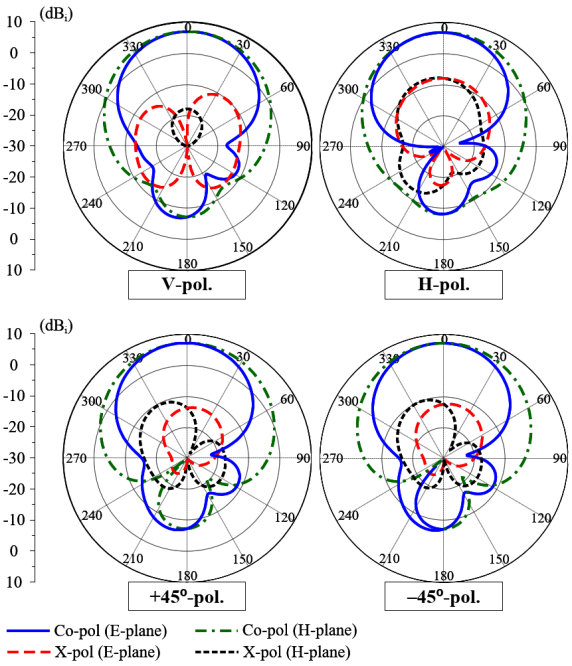

Fig. 4. Simulated gain radiation patterns at 915 MHz for different operating modes.

IV. Antenna Key Design Parameters

A. Divider Optimization

The principle to design the divider with one input and three outputs can be illustrated by observing Fig. 6. The feeding network divides one input power into three different outputs with equal magnitude. The input and output impedances are $Z_o = 50\,\Omega$. Thus, the impedance of the center point should be $Z_c = 50/3 \approx 17\,\Omega$. Finally, to match with the $50\,\Omega$ input port, a quarter-wavelength matching component is employed. The impedance of this matching component is $Z_m = \sqrt{Z_o Z_c} \approx 30\,\Omega$.

B. Diode Position

In optimizing the proposed design, the position of the PIN diodes is crucial, as it directly influences the impedance matching performance. The diode locations are selected carefully, with the distance from each diode to the central output of the power divider is denoted as $l_{d1} = l_{d2} = l_d$. Consider the case

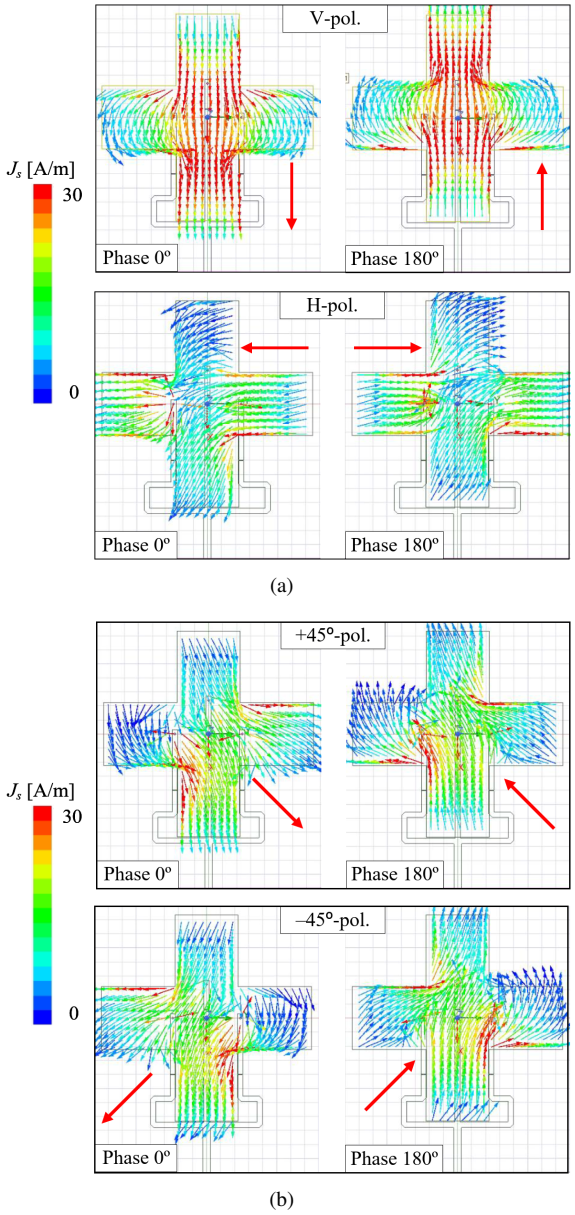

Fig. 5. Simulated surface current distribution on the crossed patch for different senses of polarizations. (a) Vertical and horizontal polarizations, (b) diagonal polarizations.

in which the antenna is configured for vertical polarization by enabling D-1 while disabling D-2 and D-3. Under this condition, the branches connected to D-2 and D-3 behave as open-ended stubs whose input impedance is given by $Z_{in} = -jZ_0 \cot(\beta l_d)$, where the phase constant is $\beta = 2\pi/\lambda_g$ [31]. To minimize the influence of these inactive branches on the active one, Z_{in} should approach infinity, which occurs when $l_d \approx \lambda_g/2$.

To illustrate this effect, Fig. 7 presents the reflection coefficient for the vertical polarization mode under different values of l_2. It is noted that varying l_2 alters the electrical distance between diodes D-2/D-3 and the divider output. The results show that l_2 strongly impacts the matching characteristics, with $l_2 = 40$ mm providing the optimal impedance match.

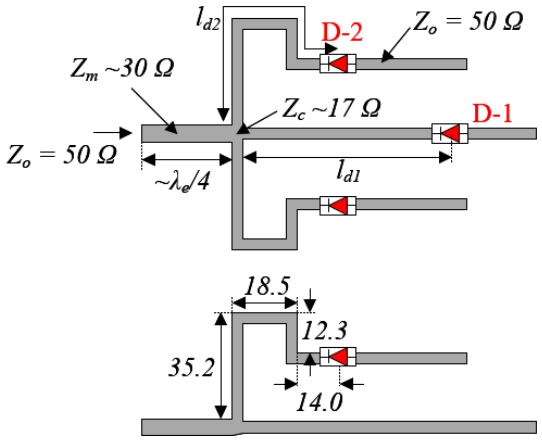

Fig. 6. Principle to design the reconfigurable feeding network.

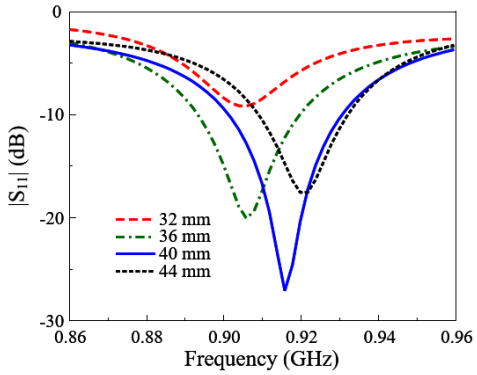

Fig. 7. Simulated $|S_{11}|$ of the vertical polarization mode for different l_2.

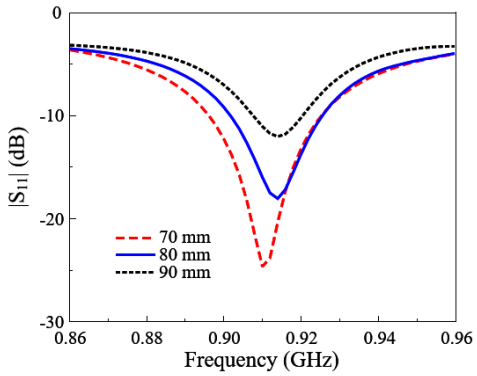

Fig. 8. Simulated $|S_{11}|$ of the horizontal polarization mode for different l_{d1}.

Similar phenomena can be observed for the horizontal polarization mode when changing the position of D-1, l_{d1}. The data in Fig. 8 indicates that changing l_{d1} has significant impact on the matching performance of the horizontal polarization mode. Here, the optimal values of l_{d1} and l_{d2} are 80 mm, which is approximately half-effective wavelength at 915 MHz calculated by equation 3.

$$\lambda_e = \frac{c}{f\sqrt{\varepsilon_{FR-4}}} \tag{3}$$

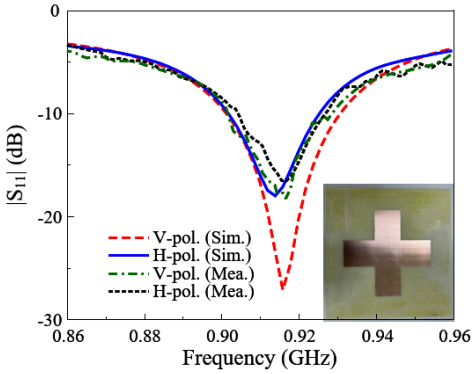

(a)

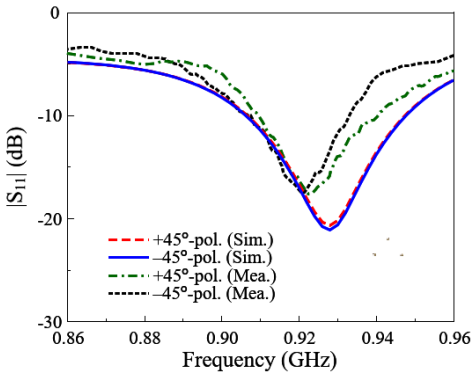

(b)

Fig. 9. Simulated and measured $|S_{11}|$ of (a) vertical and horizontal polarizations, and (b) diagonal polarizations.

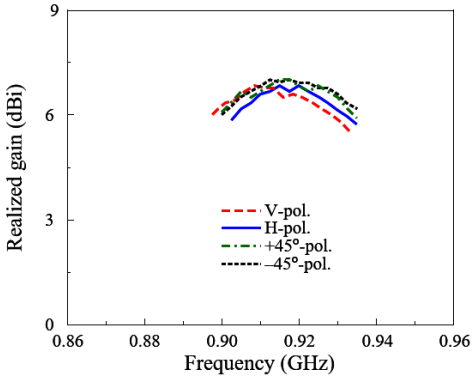

Fig. 10. Measured broadside gain for different operating modes.

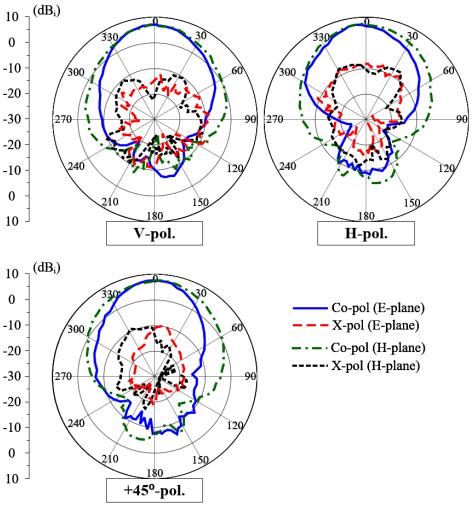

Fig. 11. Measured gain radiation patterns at 915 MHz for different operating modes.

V. Measurement Results

The proposed antenna is fabricated utilizing PCB process. The antenna is first validated with the Vector Network Analyzer and then measured in an anechoic chamber. Overall, the measured and simulated results are quite similar with a small discrepancy. It could be attributed to the tolerance in fabrication and imperfection in measurement setup.

The measured reflection coefficients for all polarization operating modes are shown in Fig. 9. The results indicate that the proposed antenna achieves good impedance matching under all reconfigurable states, with an overlapped -10 dB impedance bandwidth extending from 910 to 925 MHz, confirming the suitability of the antenna for RFID reader applications.

Within the operating band, the measured broadside realized gain remains higher than 6.2 dBi for all polarization modes, as depicted in Fig. 10, demonstrating stable radiation performance under polarization switching. The highest measured gain, approximately 6.9 dBi, is achieved in the dual-orthogonal LP modes, which can be attributed to the enhanced effective aperture utilization under this configuration.

The measured radiation patterns at the center frequency of 915 MHz in both the E- and H-planes are illustrated in Fig. 11. It is observed that the antenna exhibits highly symmetric radiation patterns for all LP modes, with well-defined main lobes directed toward the broadside. Furthermore, the measured polarization isolation between orthogonal LP states is better than 15 dB, indicating good polarization purity. The front-to-back ratio is also higher than 15 dB for all modes, which confirms the effective suppression of backward radiation and indicates good directional performance of the antenna.

VI. Performance Comparison

Firstly, a performance comparison among RFID reader antennas is summarized in Table II. It can be observed that the proposed antenna achieves superior overall performance by providing multiple polarization states together with high-gain radiation. Designs reported in [8] and [9] support only a single CP state, whereas dual-CP operation is realized in [10] and [11] at the expense of a larger number of switching diodes. Although the antenna in [17] is capable of generating four LP states, it employs larger diodes than the proposed design and still suffers from relatively low realized gain.

Secondly, a performance comparison among polarization-reconfigurable antennas is presented in Table III to further demonstrate the advantages of the proposed approach. It can be observed that achieving multiple LP states using a microstrip patch configuration is particularly challenging. Although this can be conveniently realized using dipole-based structures [15], [16], such designs typically suffer from an excessively high profile. Among polarization-reconfigurable patch antennas, most reported designs focus on dual CP and single LP

TABLE II
PERFORMANCE COMPARISON AMONG ANTENNAS FOR RFID APPLICATIONS

Ref.	Overall size (λ)	No. of diodes	Polarization states CPs	Polarization states LPs	BW (%)	Max. Gain (dBi)
[8]	$0.75 \times 0.75 \times 0.11$	0	1	0	13.5	8.6
[9]	$0.45 \times 0.45 \times 0.07$	0	1	0	9.0	7.5
[10]	N/A	2	2	0	N/A	7.2
[11]	N/A	4	2	0	0.2	6.1
[12]	$0.27 \times 0.27 \times 0.01$	1	1	1	2.4	4.1
[17]	$0.54 \times 0.54 \times 0.04$	4	0	4	1.0	2.9
Prop.	$0.67 \times 0.67 \times 0.04$	3	0	4	1.7	7.0

TABLE III
PERFORMANCE COMPARISON AMONG POLARIZATION RECONFIGURABLE PATCH ANTENNAS

Ref.	Overall size (λ)	Diodes position	No. of diodes	Polarization states CPs	Polarization states LPs	BW (%)	Max. Gain (dBi)
[18]	$0.56 \times 0.56 \times 0.07$	Radiator	4	0	4	7.1	5.9
[19]	$0.64 \times 0.64 \times 0.08$	Divider	4	0	4	17.6	6.1
[21]	$1.23 \times 1.23 \times 0.03$	Radiator	4	2	1	1.7	6.2
[23]	$1.45 \times 1.45 \times 0.07$	Radiator	2	2	1	3.2	10.6
[25]	$0.56 \times 0.56 \times 0.07$	Divider	10	2	0	6.4	7.2
[27]	$0.36 \times 0.36 \times 0.03$	Divider	2	2	1	1.2	4.8
[28]	$1.30 \times 1.30 \times 0.07$	Divider	4	2	1	17.8	9.4
Prop.	$0.67 \times 0.67 \times 0.04$	Divider	3	0	4	1.7	7.0

operation. Only a few patch-based implementations capable of generating four LP states have been reported in [18], [19], and these require a larger number of switching diodes than the proposed design.

VII. CONCLUSION

This paper presented a simple reconfigurable antenna capable of switching among four linear polarization states—horizontal, vertical, and two diagonals—using a compact feeding network controlled by only three PIN diodes. The final prototype, with overall dimensions of $220 \times 220 \times 11.6$ mm^3, operates effectively from 900 to 920 MHz, achieving broadside gains above 5.8 dBi across the band. It also exhibits symmetrical broadside radiation patterns with low cross-polarization and low back radiation. These results confirm that the proposed design is well suited for UHF RFID reader applications.

REFERENCES

[1] K. Finkenzeller, *RFID Handbook: Fundamentals and Applications in Contactless Smart Cards, Radio Frequency Identification and near-Field Communication*. Wiley, Jun. 2010. doi: 10.1002/9780470665121

[2] A. Birwal, A. Shakya, Saurav, S. Kashyap, and K. Patel, "A compact slot-based bi-directional uhf rfid reader antenna for far-field applications," *IEEE Journal of Radio Frequency Identification*, vol. 8, pp. 761–769, 2024. doi: 10.1109/jrfid.2024.3457691

[3] Z. N. Chen, X. Qing, and H. L. Chung, "A universal uhf rfid reader antenna," *IEEE Transactions on Microwave Theory and Techniques*, vol. 57, no. 5, pp. 1275–1282, 2009. doi: 10.1109/TMTT.2009.2017290

[4] M. El Bekkali, P. Singh, M. El Bakkali, L. Kansal, and G. K. Sodhi, "A low profile cpw-fed slot antenna for uhf-rfid readers," in *2021 International Conference on Computer Communication and Informatics (ICCCI)*, 2021, pp. 1–4. doi: 10.1109/ICCCI50826.2021.9402378

[5] R. Jain, V. V. Thakare, and P. K. Singhal, "Design and analysis of uwb antenna using machine learning for next-generation communications," *Cluster Computing*, vol. 28, no. 5, Apr. 2025. doi: 10.1007/s10586-024-05008-y

[6] ——, "Design and comparative analysis of thz antenna through machine learning for 6g connectivity," *IEEE Latin America Transactions*, vol. 22, no. 2, pp. 82–91, Feb. 2024. doi: 10.1109/tla.2024.10412032

[7] W. A. Ahmed and F. Quanyuan, "A novel compact cp antenna with wide axial ratio bandwidth for worldwide uhf rfid handheld reader," *International Journal of Antennas and Propagation*, vol. 2019, pp. 1–9, May 2019. doi: 10.1155/2019/2497450

[8] Z. Wang, S. Fang, S. Fu, and S. Jia, "Single-fed broadband circularly polarized stacked patch antenna with horizontally meandered strip for universal uhf rfid applications," *IEEE Transactions on Microwave Theory and Techniques*, vol. 59, no. 4, pp. 1066–1073, 2011. doi: 10.1109/TMTT.2011.2114010

[9] J. Li, H. Liu, S. Zhang, M. Luo, Y. Zhang, and S. He, "A wideband single-fed, circularly-polarized patch antenna with enhanced axial ratio bandwidth for uhf rfid reader applications," *IEEE Access*, vol. 6, pp. 55 883–55 892, 2018. doi: 10.1109/ACCESS.2018.2872692

[10] J. Shen, C. Wu, E. Fang, X. Liu, H. Cao, W. Zhang, and K.-W. Tam, "Autoreconfigurable circular polarization antenna for enhanced rfid coverage," *IEEE Antennas and Wireless Propagation Letters*, vol. 22, no. 12, pp. 2955–2959, 2023. doi: 10.1109/LAWP.2023.3306385

[11] H. Aissat, L. Cirio, M. Grzeskowiak, J.-M. Laheurte, and O. Picon, "Reconfigurable circularly polarized antenna for short-range communication systems," *IEEE Transactions on Microwave Theory and Techniques*, vol. 54, no. 6, pp. 2856–2863, 2006. doi: 10.1109/TMTT.2006.875454

[12] Y. F. C. X. Ding, W. Shao, T. L. Liang, B. Z. Wang, and D. E. Anagnostou, "A polarization reconfigurable rfid reader antenna," in *2017 IEEE International Symposium on Antennas and Propagation & USNC/URSI National Radio Science Meeting*, 2017, pp. 2213–2214. doi: 10.1109/APUSNCURSINRSM.2017.8073149

[13] D. Duraj, K. Nyka, and M. Rzymowski, "Dual polarization antennas for uhf rfid readers," in *2014 20th International Conference on Microwaves, Radar and Wireless Communications (MIKON)*, 2014, pp. 1–4. doi: 10.1109/MIKON.2014.6899830

[14] P. Parthiban, B.-C. Seet, and X. J. Li, "Low-cost low-profile uhf rfid reader antenna with reconfigurable beams and polarizations," in *2017 IEEE International Conference on RFID (RFID)*, 2017, pp. 81–87. doi: 10.1109/RFID.2017.7945591

[15] S. Yu, K. Yang, and Y. Zhang, "A wideband multi-linear polarization reconfigurable antenna with artificial magnetic conductor," *Electronics*, vol. 14, no. 21, p. 4170, Oct. 2025. doi: 10.3390/electronics14214170
[16] K. Yang, N. Kou, and S. Yu, "Wideband multi-linear polarization reconfigurable antenna for wireless communication system," *Progress In Electromagnetics Research Letters*, vol. 117, pp. 75–81, 2024. doi: 10.2528/pierl23112403
[17] E. Tolin, F. Vipiana, S. Bruni, and A. Bahr, "Polarization reconfigurable patch antenna for compact and low cost uhf rfid reader," in *2019 IEEE International Conference on RFID Technology and Applications (RFID-TA)*, 2019, pp. 128–130. doi: 10.1109/RFID-TA.2019.8892109
[18] S.-L. Chen, F. Wei, P.-Y. Qin, Y. J. Guo, and X. Chen, "A multi-linear polarization reconfigurable unidirectional patch antenna," *IEEE Transactions on Antennas and Propagation*, vol. 65, no. 8, pp. 4299–4304, 2017. doi: 10.1109/TAP.2017.2712185
[19] W. Lin and H. Wong, "Multipolarization-reconfigurable circular patch antenna with l-shaped probes," *IEEE Antennas and Wireless Propagation Letters*, vol. 16, pp. 1549–1552, 2017. doi: 10.1109/LAWP.2017.2648862
[20] S. W. Lee and Y. J. Sung, "Simple polarization-reconfigurable antenna with t-shaped feed," *IEEE Antennas and Wireless Propagation Letters*, vol. 15, pp. 114–117, 2016. doi: 10.1109/LAWP.2015.2432462
[21] J. L. Valdes, L. Huitema, E. Arnaud, D. Passerieux, and A. Crunteanu, "A polarization reconfigurable patch antenna in the millimeter-waves domain using optical control of phase change materials," *IEEE Open Journal of Antennas and Propagation*, vol. 1, pp. 224–232, 2020. doi: 10.1109/OJAP.2020.2996767
[22] Y. Zhang, Y. Zhang, K. Huang, S.-J. Liu, X. Y. Zhang, and Q. H. Liu, "A reconfigurable patch antenna with linear and circular polarizations based on double-ring-slot feeding structure," *IEEE Transactions on Antennas and Propagation*, vol. 70, no. 12, pp. 11 389–11 400, 2022. doi: 10.1109/TAP.2022.3209185
[23] Q. Chen, J.-Y. Li, G. Yang, B. Cao, and Z. Zhang, "A polarization-reconfigurable high-gain microstrip antenna," *IEEE Transactions on Antennas and Propagation*, vol. 67, no. 5, pp. 3461–3466, 2019. doi: 10.1109/TAP.2019.2902750
[24] J. Yang, J. Li, S. Zhou, D. Li, and G. Yang, "A polarization and frequency reconfigurable microstrip antenna for vehicular communication system application," *IEEE Transactions on Vehicular Technology*, vol. 72, no. 1, pp. 623–631, 2023. doi: 10.1109/TVT.2022.3202973
[25] C. Liu, Y. Li, T. Liu, Y. Han, J. Wang, and S. Qu, "Polarization reconfigurable and beam-switchable array antenna using switchable feed network," *IEEE Access*, vol. 10, pp. 29 032–29 039, 2022. doi: 10.1109/ACCESS.2022.3153393
[26] T. Nguyen-Dinh, H. Nguyen-Tuan, H. Tran-Huy, D. Nguyen-Quoc, and N. Nguyen-Trong, "A simple polarization-reconfigurable series-fed patch array using switchable feeding network," *IEEE Antennas and Wireless Propagation Letters*, vol. 23, no. 9, pp. 2658–2662, 2024. doi: 10.1109/LAWP.2024.3403880
[27] T. Nguyen-Dinh, T. Dao-Duc, D. Nguyen-Quoc, H. Tran-Huy, and N. Hussain, "A method to design polarization reconfigurable antenna with simple switching mechanism and compact size characteristics," *Scientific Reports*, vol. 15, no. 1, Apr. 2025. doi: 10.1038/s41598-025-97908-1
[28] J. Hu, G. Q. Luo, and Z.-C. Hao, "A wideband quad-polarization reconfigurable metasurface antenna," *IEEE Access*, vol. 6, pp. 6130–6137, 2018. doi: 10.1109/ACCESS.2017.2766231
[29] W. Lin and H. Wong, "Wideband circular-polarization reconfigurable antenna with l-shaped feeding probes," *IEEE Antennas and Wireless Propagation Letters*, vol. 16, pp. 2114–2117, 2017. doi: 10.1109/LAWP.2017.2699289
[30] MACOM, "Madp-042305-130600 product detail," https://www.macom.com/products/product-detail/MADP-042305-130600, 2025, accessed: 25 Nov. 2025.
[31] D. M. Pozar, *Microwave engineering*, fourth edition ed. Hoboken, NJ: John Wiley & Sons, Inc., 2012, enthält Übungsaufgaben.

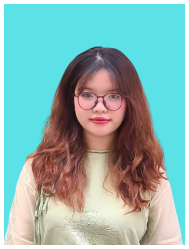

Trang Hoang-Thu is an undergraduate student at Faculty of Electrical and Electronic Engineering, Phenikaa School of Engineering, Phenikaa University, Hanoi, Vietnam. Her research interests have included microstrip patch antennas, MIMO antennas, and microwave technology.

Hung Pham-Duy received the B.E. degree in Electronics and Telecommunications from the Hanoi University of Science and Technology (HUST), Hanoi, Vietnam, in 2015. He is currently a Research Assistant with the Faculty of Electrical and Electronic Engineering at Phenikaa University, Hanoi. His current research interests include the design and optimization of microstrip patch antennas, specifically focusing on wideband enhancement techniques using U-slots and V-cut geometries. Additionally, his work explores circular polarization, metasurfaces, and the development of MIMO systems for 5G applications.

Hung Tran-Huy received the B.S. degree in electronics and telecommunications from Hanoi University of Science and Technology, Hanoi, Vietnam, in 2013. He received his M.S. and Ph. D. degrees in electrical engineering from Ajou University, in 2015, and Dongguk University, Korea, in 2020, respectively. He is currently a lecturer at Faculty of Electrical and Electronic Engineering, PHENIKAA School of Engineering, PHENIKAA University, Hanoi, Vietnam. His research interests have included circularly polarized antennas, MIMO antennas, metamaterial-based antennas, and reconfigurable antennas.

Hyun-Chang Park (Member, IEEE) received the B.S. degree in electronics engineering from Seoul National University, Seoul, South Korea, in 1986, and the M.S. and Ph.D. degrees in electrical engineering from Cornell University, Ithaca, NY, USA, in 1989 and 1993, respectively. From 1993 to 1995, he was a Research Associate with the Department of Electrical Engineering, University of Virginia, Charlottesville, VA, USA. In 1995, he joined the Department of Electronics and Electrical Engineering, Dongguk University, Seoul, South Korea, where he is currently a Professor. His research interests include RF energy harvesting, wideband/multi-band planar antennas, and reconfigurable antennas for various wireless applications.